PHYSICAL REVIEW A VOLUME 18, NUMBER 4 OCTOBER 1978

General theory of laser-induced quantum beats. II. Sequential laser excitation; effects of external static fields

M. P. Silverman
Department of Physics, Wesleyan University, Middletown, Connecticut 06457

S. Haroche and M. Gross
Laboratoire de Spectroscopie Hertzienne de l'Ecole Normale Supérieure, 75321 Paris Cédex 05, France
(Received 21 July 1977)

A general theory of laser-induced quantum beats introduced in paper I is extended to include the effects of sequential laser excitation by several lasers for atomic systems either free or subjected to external static fields. A detailed study is made of the dependence of the quantum beat signal on the polarizations of the exciting laser pulses and detected spontaneous emission. The theory is applied to the echelon excitation of sodium *nD* Rydberg states. An analysis of the Zeeman beats produced by excitation in an external magnetic field suggests new ways to measure the fine-structure interaction constant of the Rydberg levels.

I. INTRODUCTION

In paper I[1] we considered the dynamical aspects of atomic excitation by a single-pulsed laser and the variations of the quantum-beat signal as a function of laser intensity. Specific saturation effects resulting from stimulated emission from the excited atomic states during passage of the laser pulse and light-induced level shifts were studied in detail. There still remain to be discussed those geometrical aspects of the laser-induced quantum-beat effect concerned with the polarizations of the exciting light pulses and the detected fluorescence. It is well known that the modulation depth and phase of the beats are strongly dependent on the directions of these polarizations.

In this article we discuss the polarization dependence of the quantum-beat signal for the general case of laser excitation in echelon (i.e., sequential excitation by more than one laser) starting from a nonoriented atomic ground state. The experimental significance of this stepwise excitation process is that it permits one to reach highly energetic atomic states lying close to the ionization limit (Rydberg states). Depending on the number of sequential excitations, states of either odd or even parity can be populated regardless of the ground-state parity. In order to bring out clearly the physical principles involved, we will discuss in detail the simplest case of two-laser excitation. Our theory, however, is expressed in a formalism easily generalized to include more complex cases.

This article is divided into two main parts. In the first part we derive general expressions for the angular dependence of the quantum-beat signal in the absence of external static electric or magnetic fields. In order to separate clearly the geometric problems associated with the polarizations of the laser and fluorescent light from the complicating features of laser saturation, we will consider first the linear or weak-pumping approximation. We have shown in paper I that this approximation is generally quite satisfactory. The general theory that we develop will be applied to the specific case of sodium atoms sequentially excited into the *nD* levels via the intermediate $3P_{3/2}$ level. This example is of particular experimental interest because of the inverted ordering of the *D* fine structure and has been recently studied in much detail by laser-induced quantum-beat spectroscopy.[2] We will also analyze this experiment using the full rigor of the general theory to show what modifications in the weak-pumping approximation result from laser saturation.

In the second part we extend the theory to include the effects of external static fields on the quantum-beat signal. The results of this calculation suggest new experimental methods for measuring internal interaction constants of Rydberg states.

II. SEQUENTIAL LASER EXCITATION IN THE ABSENCE OF EXTERNAL FIELDS

A. Determination of the quantum-beat signal in the weak-pumping approximation

In Fig. 1 is shown a general level diagram of a four-level atom illustrating the echelon excitation and quantum-beat detection processes. Two time-delayed laser pulses of polarization $\hat{\epsilon}_1$ and $\hat{\epsilon}_2$, respectively, bring the atom from the ground state 0 to the excited state 2 via the intermediate state 1. As a consequence of the coherent population of the sublevels of 2, the intensity of the light (detected with polarization $\hat{\epsilon}_d$) resulting from the subsequent transition from 2 to *f* will be modulated.

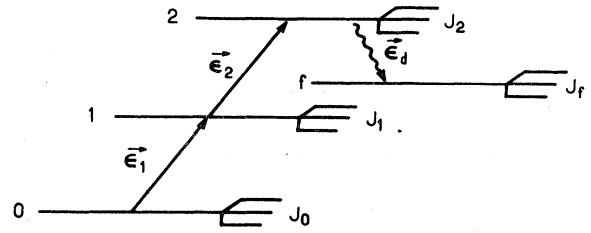

FIG. 1. Schematic diagram for two-laser echelon excitation. $\hat{\epsilon}_1$ and $\hat{\epsilon}_2$ characterize the polarization of the laser pulses. Quantum beats are observed on the J_2–J_f transition with a polarization $\hat{\epsilon}_d$.

The atom is not subjected to any external fields. The energy-level structure, therefore, depends only on the angular momenta of the different substates. In what follows we consider only internal interactions of the type $\vec{L}\cdot\vec{S}$ in order to calculate the fine-structure quantum-beat signal. Hyperfine structure is assumed to be negligible. Each level i ($i=0,1,2,f$) is labeled by the orbital angular momentum L_i, the total electron angular momentum J_i, and the projection m_i of the total momentum on some arbitrary axis to be specified later. S is the spin angular momentum common to all the states. The results derived in this section can be easily generalized to include hyperfine structure by substituting $L_i \to J_i$, $S \to I$. We will not consider in this article the more complex case where fine and hyperfine structures are of the same order of magnitude.

The notation describing the partial-density matrix of each electronic manifold is a simple extension of that introduced in paper I. σ_i^+ is the partial-density matrix of level i immediately following laser excitation from level $i-1$. For the nonoriented ground state we write

$$\sigma_0^+ = P_0 ,$$

where P_0 is the projection operator onto the ground state. We further assume that the duration and spacing of the successive optical pulses are very short in comparison to the Bohr precession periods within the various levels. *Each* excitation is therefore essentially instantaneous and *all* excitations occur essentially at the same instant. No significant evolution of the quantum states takes place during the excitation processes.

Given the above circumstances, the density-matrix equations (I6a) and (I6b)[3] of paper I solved in the weak-pumping approximation can be used to give the partial-density matrix σ_i^+ in terms of the partial-density matrix of the previous level σ_{i-1}^+:

$$\sigma_i^+ = k_0^{(i)}(+\infty) P_i \hat{\epsilon}_i \cdot \vec{D} P_{i-1} \sigma_{i-1}^+ P_{i-1} \hat{\epsilon}_i^* \cdot \vec{D} P_i , \quad \text{(1a)}$$

where

$$k_0^{(i)}(+\infty) = \int_{-\infty}^{\infty} \frac{dt'}{T_p^{(i)}(t')} . \quad \text{(1b)}$$

Equation (1) allows one to deduce σ_1^+ from σ_0^+ and σ_2^+ from σ_1^+. Knowledge of σ_2^+ yields the quantum-beat signal through use of Eq. (I1).

For even a relatively simple atomic system such as that of an alkali atom, there is a multiplicity of sublevels all of which may contribute to the quantum-beat signal. The explicit determination of this signal would be a rather formidable task were it not possible to circumvent tedious series summations through use of irreducible tensor operators.[4] The simple rotational properties of these operators allow one to write the signal as a sum of a small number of terms each having the angular dependence of a spherical harmonic or of a product of two spherical harmonics. We therefore introduce for each level i a base of irreducible tensor operators

$$ {}^{J_i J_i'}T_{q_i}^{k_i} = \sum_{m_i m_i'} (2k_i+1)^{1/2} (-1)^{J_i - M_i} \times |J_i m_i\rangle\langle J_i' m_i'| \begin{pmatrix} J_i & k_i & J_i' \\ -m_i & q_i & m_i' \end{pmatrix} . \quad \text{(2)}$$

Each of these operators acts only within the ith manifold of states and only between J_i and J_i'. This leads to the following expression for the time evolution of ${}^{J_i J_i'}T_{q_i}^{k_i}$:

$$\exp(-i\mathcal{H}_0 t/\hbar)\, {}^{J_i J_i'}T_{q_i}^{k_i} \exp(+i\mathcal{H}_0 t/\hbar) = \exp(-i\omega_{J_i J_i'} t)\, {}^{J_i J_i'}T_{q_i}^{k_i} . \quad \text{(3)}$$

The tensor operators obey the following orthogonality relation

$$\mathrm{Tr}\{ {}^{J J'}T_q^{k\,\dagger}\, {}^{J'' J'''}T_{q'}^{k'}\} = \delta_{J J''}\delta_{J' J'''}\delta_{k k'}\delta_{q q'} , \quad \text{(4)}$$

and transform under rotation according to the characteristic equation

$$\mathcal{R}(\phi,\theta,\gamma)\, {}^{J_i J_i'}T_{q_i}^{k_i} \mathcal{R}^{-1}(\phi,\theta,\gamma) = \sum_{q'} R_{q' q_i}^{(k_i)}\, {}^{J_i J_i'}T_{q'}^{k_i} . \quad \text{(5)}$$

A compact expression for the quantum-beat signal which clearly exhibits its geometric properties is obtained by expanding the partial density matrices and the detection operator [Eq. (I2)] in the base of irreducible tensor operators. We consider first the partial density matrix σ_i^+ representable as

$$\sigma_i^+ = \sum \alpha_{k_i q_i}^{J_i J_i'}\, {}^{J_i J_i'}T_{q_i}^{k_i} , \quad \text{(6a)}$$

where

$$\alpha_{k_i q_i}^{J_i J_i'} = \mathrm{Tr}\{\sigma_i^+\, {}^{J_i J_i'}T_{q_i}^{k_i\,\dagger}\} . \quad \text{(6b)}$$

For the nonoriented ground state we have

$$\sigma_0^+ = \frac{1}{(2J_0+1)^{1/2}}\, {}^{J_0 J_0} T_0^0 . \tag{6c}$$

Equation (1), which expresses σ_i^+ in terms of σ_{i-1}^+, leads to a linear relation between the coefficients α of level i and those of level $i-1$

$$\alpha^{J_i J_i'}_{k_i q_i} = k_0^{(i)}(+\infty) \sum {}^{J_i J_i'}_{k_i q_i} A^{J_{i-1} J_{i-1}'}_{k_{i-1} q_{i-1}} (\hat{\epsilon}_1)\, \alpha^{J_{i-1} J_{i-1}'}_{k_{i-1} q_{i-1}} . \tag{7}$$

The explicit expression for the transformation coefficients A will be given and discussed shortly. A derivation of this expression can be found in Ref. 5. These coefficients obey the selection rule $|k_i - k_{i-1}| \leq 2$ and the symmetry relation

$$({}^{J_i J_i'}_{k_i q_i} A^{J_j J_j'}_{k_j q_j}(\hat{\epsilon}))^* = {}^{J_j J_j'}_{k_j q_j} A^{J_i J_i'}_{k_i q_i}(\hat{\epsilon}^*) . \tag{8}$$

For the case of two-laser excitations the α coefficients of the state 2 are obtained from the recursion relation (7) and the ground-state density matrix (6c):

$$\alpha^{J_2 J_2'}_{k_2 q_2} = k_0^{(1)}(+\infty) k_0^{(2)}(+\infty) \times \sum \frac{1}{(2J_0+1)^{1/2}}\, {}^{J_2 J_2'}_{k_2 q_2} A^{J_1 J_1'}_{k_1 q_1}(\hat{\epsilon}_2)\, {}^{J_1 J_1'}_{k_1 q_1} A^{J_0 J_0}_{00}(\hat{\epsilon}_1) . \tag{9}$$

We now consider the expansion of the detection operator $\theta_{\text{det}}(\hat{\epsilon}_d)$ given in paper I as

$$\theta_{\text{det}} = P_2 \hat{\epsilon}_d \cdot \vec{D} P_f \hat{\epsilon}_d^* \cdot \vec{D} P_2 \tag{10}$$

in the base of irreducible tensor operators:

$$\theta_{\text{det}} = \sum \beta^{J_2'' J_2'''}_{k_2' q_2'}\, {}^{J_2'' J_2'''} T^{k_2'}_{q_2'} . \tag{11}$$

Examination of Eq. (1a) and (11) shows that θ_{det} is related to P_f, the projection operator onto the final state f, by a linear relation of identical mathematical form to the one connecting σ_1^+ to σ_0^+. The expression for the β coefficients is therefore immediately deducible in terms of the known A coefficients:

$$\beta^{J_2'' J_2'''}_{k_2' q_2'} = (2J_f+1)^{-1/2}\, {}^{J_2'' J_2'''}_{k_2' q_2'} A^{J_f J_f}_{00}(\hat{\epsilon}_d) . \tag{12}$$

The quantum-beat signal $I(\hat{\epsilon}_d)$ adopted from Eq. (I5) can be written as

$$I(\hat{\epsilon}_d) = \text{Tr}\{P_2 e^{-i\mathcal{H}_0 t/\hbar} \sigma_2^+ e^{+i\mathcal{H}_0 t/\hbar} \theta_{\text{det}}^\dagger\}\, e^{-\Gamma t} . \tag{13}$$

By combining the tensor expansions of θ_{det} [Eqs. (11) and (12)] and of σ_2^+ [Eqs. (6a), (6b), and (9)], the symmetry relation [Eq. (8)], the orthogonality relation [Eq. (4)], and the field-free time development of the irreducible tensors [Eq. (3)], one obtains the following multipolar form for the quantum-beat signal:

$$I = k_0^{(1)}(+\infty) k_0^{(2)}(+\infty) \times \sum {}^{J_f J_f} A^{J_2 J_2'}_{00}\, {}^{J_2 J_2'}_{k_2 q_2}(\hat{\epsilon}_d^*)\, {}^{J_2 J_2'}_{k_2 q_2} A^{J_1 J_1'}_{k_1 q_1}(\hat{\epsilon}_2)\, {}^{J_1 J_1'}_{k_1 q_1} A^{J_0 J_0}_{00}(\hat{\epsilon}_1) \times [(2J_f+1)(2J_0+1)]^{-1/2} e^{-i\omega_{J_2 J_2'} t} e^{-\Gamma t} . \tag{14}$$

The mathematical structure of this expression is actually quite simple. There is a sum over products of three A coefficients which, from right to left, characterize the three successive transitions undergone by the atoms during the course of the experiment: excitation from level 0 to level 1, excitation from level 1 to level 2, and decay from level 2 to level f. Each A coefficient contains the entire angular dependence of the corresponding transition.

The amplitude of the modulation at each frequency $\omega_{J_2 J_2'}$ is obtained by summing over the repeated indices in Eq. (14). The sum over the tensor orders k_1 and k_2 is restricted by the selection rule $\Delta k_i \leq 2$ to include only the values 0, 1, and 2. The sum over the component index q_i ranges from $-k_i$ to $+k_i$ in integral steps. The sum over the angular momenta J_0, J_1, J_1', and J_f is determined by each experimental situation. In the case that the first laser pulse has a spectral bandwidth Δ_1 greater than the fine structure of levels 0 and 1, one induces transitions from all the levels J_0 to all the possible levels J_i of the intermediate state. If the fine structure in the state 0 or 1 is greater than Δ_1, then only certain of the J_0-J_1 transitions are induced and the summation is accordingly restricted. Likewise, only those quantum numbers J_f are included for which the appropriate radiative decay transitions are detected.

B. Angular dependence of the signal

In this section we discuss the polarization dependence of the A coefficients in order to obtain an explicit expression for the angular dependence of the beat signal. We restrict our study to linear and circular polarizations. The polarization of an electric field can be completely characterized by the Euler angles θ, ϕ of the unit vector which specifies the direction of field oscillation (for linear polarization) or the axis of field rotation (for circular polarization). (See Fig. 2.) If $\theta = \phi = 0$ we refer to the polarization as one of three "principal polarizations": π if $\hat{\epsilon}$ is linear along the $0Z$ axis, and σ_+ or σ_- if $\hat{\epsilon}$ rotates in the $X0Y$ plane counterclockwise or clockwise, respectively.

In the case of a principal polarization the A coefficients, derived in Ref. 5, take the following form:

$$
{}^{J_i J_i'}_{k_i q_i} A^{J_{i-1} J_{i-1}'}_{k_{i-1} q_{i-1}}(Q_i) = (-1)^{2(L_i+S)+1}(-1)^{(J_i+J_i')}(-1)^{k_i+q_i+Q_i}\delta_{q_i q_{i-1}}
$$

$$
\times[(2k_i+1)(2k_{i-1}+1)(2J_i+1)(2J_i'+1)(2J_{i-1}+1)(2J_{i-1}'+1)]^{1/2}
$$

$$
\times\begin{Bmatrix} L_i & 1 & L_{i-1} \\ J_{i-1} & S & J_i \end{Bmatrix}\begin{Bmatrix} L_i & 1 & L_{i-1} \\ J_{i-1}' & S & J_i' \end{Bmatrix}
$$

$$
\times\sum_{x=0,1,2}(2x+1)\begin{pmatrix} 1 & 1 & x \\ Q_i & -Q_i & 0 \end{pmatrix}\begin{pmatrix} x & k_{i-1} & k_i \\ 0 & -q_{i-1} & q_i \end{pmatrix}\begin{Bmatrix} 1 & 1 & 1 \\ J_{i-1} & J_{i-1}' & k_{i-1} \\ J_i & J_i' & k_i \end{Bmatrix}. \tag{15}
$$

The index Q_i is equal to 0, +1, or −1 if the excitation polarization is respectively π, σ_+, or σ_-. $\delta_{q_i q_{i-1}}$, the Kronecker δ symbol, expresses the fact that the excitation is rotationally invariant about the $0Z$ axis and therefore cannot couple tensor operators T^k_q with different q. The various $3J$ and $6J$ symbols impose certain selection rules. In particular the $3J$,

$$
\begin{pmatrix} 1 & 1 & x \\ Q & -Q & 0 \end{pmatrix},
$$

is nonzero only if $x = 0, 1, 2$. This restriction, applied to the other $3J$,

$$
\begin{pmatrix} x & k_{i-1} & k_i \\ 0 & -q_{i-1} & q_i \end{pmatrix},
$$

leads to the previously mentioned selection rule $|k_{i-1} - k_i| \leq 2$ characteristic of electric dipole transitions. Finally, utilization of the symmetry properties of the $3J$, $6J$, and $9J$ symbols leads to the following symmetry property of the A coefficients:

$$
{}^{J_i J_i'}_{k_i q_i} A^{J_{i-1} J_{i-1}'}_{k_{i-1} q_{i-1}}(Q_i) = {}^{J_{i-1} J_{i-1}'}_{k_{i-1} q_{i-1}} A^{J_i J_i'}_{k_i q_i}(-Q_i). \tag{16}
$$

The above relation is recognized as a special case of Eq. (8) since A is real for a principal polarization.

The expression for the A coefficients in the general case of arbitrary polarization $\hat{\epsilon}_i$ defined by the Euler angles θ_i, ϕ_i is easily deduced from the A coefficients for the principal polarizations by making use of the rotational properties of the irreducible tensors. This is accomplished by carrying out two rotations. A first rotation $\mathcal{R}^{-1}(\phi_i, \theta_i, 0)$ on the operator $T^{k_{i-1}}_{q_{i-1}}$ brings $\hat{\epsilon}_i$ into the direction of $0Z$ thereby making it a principal polarization. We can now define the polarization component Q_i and use the known coefficients $A(Q_i)$ to characterize the passage from $T^{k_{i-1}}_{q_{i-1}}$ to $T^{k_i}_{q_i}$. A second rotation $\mathcal{R}(\phi_i, \theta_i, 0)$ on the $T^{k_i}_{q_i}$ returns the polarization $\hat{\epsilon}_i$ to its initial position. The final expression for $A(\hat{\epsilon}_i)$ obtained by these rotational transformations is

$$
{}^{J_i J_i'}_{k_i q_i} A^{J_{i-1} J_{i-1}'}_{k_{i-1} q_{i-1}}(Q_i, \theta_i, \phi_i)
$$

$$
= \sum_q R^{(k_i)}_{q_i q}(\phi_i, \theta_i, 0)\ {}^{J_i J_i'}_{k_i q} A^{J_{i-1} J_{i-1}'}_{k_{i-1} q}(Q_i)
$$

$$
\times[R^{(k_{i-1})}(\phi_i, \theta_i, 0)]^{(-1)}_{q\, q_{i-1}}. \tag{17}
$$

To illustrate angular dependence explicitly, we replaced the notation $A(\hat{\epsilon}_i)$ by $A(Q_i, \theta_i, \phi_i)$.

A general expression for the quantum-beat signal is obtained by combining Eqs. (14) and (17). The signal is independent of the choice of the $0Z$ axis although a judicious choice could simplify the mathematical form. We take, for the moment, $0Z$ parallel to $\hat{\epsilon}_2$, i.e., $\theta_2 = \phi_2 = 0$. This leads to

$$
I = k_0^{(1)}(+\infty) k_0^{(2)}(+\infty) \sum[(2J_0+1)(2J_f+1)]^{-1/2} e^{-i\omega_{J_2 J_2'} t} e^{-\Gamma t}\ {}^{J_f J_f}_{00} A^{J_2 J_2'}_{k\,0}(-Q_d)
$$

$$
\times[R^{(k_2)}(\phi_d, \theta_d, 0)]^{(-1)}_{0 q_2}\ {}^{J_2 J_2'}_{k_2 q_2} A^{J_1 J_1'}_{k_1 q_1}(Q_2)\, R^{(k_1)}_{q_1 0}(\phi_1, \theta_1, 0)\ {}^{J_1 J_1'}_{k_1 0} A^{J_0 J_0}_{00}(Q_1). \tag{18}
$$

Q_1, Q_2, and Q_d are equal to 0, ±1 depending on whether the corresponding polarization is linear or circular. The angular dependence of the signal is entirely contained in the rotation matrix elements $R^{(k_i)}_{q_i 0}$ which are proportional to spherical harmonics.

C. Application to sodium *nD* Rydberg states

The general expression, Eq. (18), for the quantum-beat signal issued by an atom subjected to a two-step laser excitation process is algebraically complex and its geometrical properties not easily

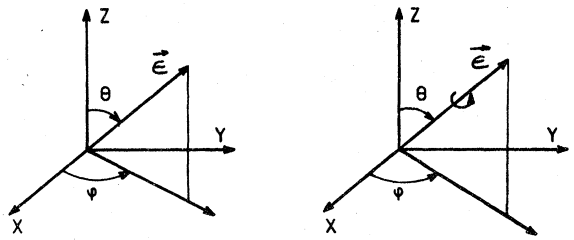

FIG. 2. A unit polarization vector is specified by the Euler angles of the axis of (a) electric field oscillation (for linear polarization) or (b) rotation (for circular polarization). The sense of rotation about an axis is given by the right-hand rule.

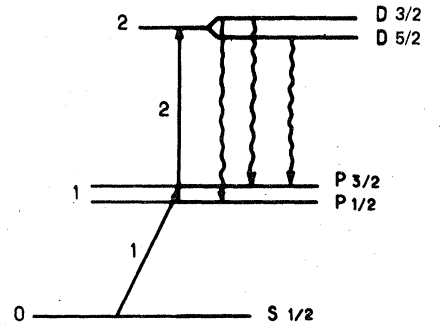

FIG. 3. Level diagram for the echelon excitation of sodium nD Rydberg states from the $3S_{1/2}$ ground state via the $3P_{3/2}$ intermediate state.

inferred. To illustrate some of the physical ideas contained in this expression we use it to discuss a recently performed experiment on the nD Rydberg states of the sodium atom.[2]

In Fig. 3 are shown the specific excitation and detection processes under consideration. Two-laser pulses excite the atom from the $3S_{1/2}$ ground state to the $nD_{5/2,3/2}$ excited states via the intermediate $3P_{3/2}$ state. Since the fine-structure interval in the $3P$ level (17 cm^{-1}) is much larger than the spectral bandwidth of the lasers (~1 cm^{-1}), it is possible to select only one of the P-level fine-structure components. The fluorescent radiation upon which are superposed the quantum beats is detected for the nD to $3P$ transition. The detection is made without a monochromator and therefore transitions to both the $P_{3/2}$ and $P_{1/2}$ states are detected. In summary, we must therefore employ in Eq. (18) the following angular-momentum quantum numbers:

$$J_0=\tfrac{1}{2};\quad J_1=J_1'=\tfrac{3}{2};\quad J_2,J_2'=\tfrac{3}{2}\text{ and }\tfrac{5}{2},\quad J_f=\tfrac{1}{2}\text{ and }\tfrac{3}{2}.$$

In the case of linear excitation and detection polarization, evaluation of Eq. (18) leads to the signal (in arbitrary units)

$$I=I_0+I_m\cos\omega_{FS}t\,, \tag{19a}$$

where

$$\begin{aligned}I_0 &= 148.148\\ &+66.369\,[\tfrac{1}{2}(3\cos^2\theta_d-1)]+14.814\,[\tfrac{1}{2}(3\cos^2\theta_1-1)]\\ &+63.703\,[\tfrac{1}{2}(3\cos^2\theta_d-1)]\,[\tfrac{1}{2}(3\cos^2\theta_1-1)]\\ &+105.333\sin2\theta_1\sin2\theta_d\cos(\phi_1-\phi_d)\\ &+67.333\sin^2\theta_1\sin^2\theta_d\cos2(\phi_1-\phi_d)\,,\end{aligned} \tag{19b}$$

and

$$\begin{aligned}I_m &= 37.333\,[\tfrac{1}{2}(3\cos^2\theta_d-1)]\\ &-26.666\,[\tfrac{1}{2}(3\cos^2\theta_1-1)][\tfrac{1}{2}(3\cos^2\theta_d-1)]\\ &-38.666\sin2\theta_1\sin2\theta_d\cos(\phi_1-\phi_d)\\ &-8.666\sin^2\theta_1\sin^2\theta_d\cos2(\phi_1-\phi_d)\,.\end{aligned} \tag{19c}$$

The frequency ω_{FS} characterizes the fine-structure splitting in the nD level.

Table I summarizes the values obtained for I_0, I_m, and the modulation depth $\eta_0=I_m/I_0$ for different polarization configurations. We disregard for the time being the last column of the table. The first two lines and last three lines in the table correspond, respectively, to the cases of parallel and perpendicular laser polarizations. For each of these two excitation configurations there are various simple configurations of detection polarization.

An examination of Table I immediately reveals several important facts. First is a verification of the relations

$$\begin{aligned}&I_m(I)+2I_m(II)=0\,,\\ &I_m(III)+I_m(IV)+I_m(V)=0\,,\end{aligned} \tag{20}$$

which express simply that the quantum beats vanish when, for each excitation configuration, signals of three orthogonal polarizations are detected simultaneously. This result is characteristic of all experiments in which the signal is sensitive to nondiagonal elements of the atomic density matrix (the coherence terms). To observe these coherences there must be a privileged detection polarization. The detection of all polarizations gives a signal sensitive only to the populations of the excited states. Neither quantum beats nor level crossings would be detected under such conditions.

In order that the sum rule, Eq. (20), be satisfied it is necessary that the quantum beats undergo a 180° shift in phase when one passes from configuration I to II, or from configuration III to IV or V. This is a very useful experimental property in that it allows one to verify that observed modulations are indeed of atomic origin. Moreover, the measurement of the difference of two signals in phase opposition enhances the beat contrast by eliminat-

TABLE I. Coefficients I_0, I_m, of the signal- and beat-modulation depth η for various polarization configurations, in the case of fine-structure quantum beats of the nD states of Na induced by stepwise laser excitation. Two values of η are given. η_0 corresponds to the weak-pumping case; η_S corresponds to the strong-pumping limit. I_0 and I_m values given in the table result from the weak-pumping limit calculation.

	Polarization configuration	Value of θ, ϕ	I_0	I_m	η_0	η_S
I	$\updownarrow_{\epsilon_1}$ $\updownarrow_{\epsilon_2}$ $\updownarrow_{\epsilon_d}$	$\theta_1=\phi_1=0$ $\theta_d=\phi_d=0$	293.035	10.666	3.64%	3.64%
II	$\updownarrow_{\epsilon_1}$ $\updownarrow_{\epsilon_2}$ $\leftrightarrow_{\epsilon_d}$	$\theta_1=\phi_1=0$ $\theta_d=\pi/2$, $\phi_d=0$	97.926	−5.333	−5.44%	−5.44%
III	$\leftrightarrow_{\epsilon_1}$ $\updownarrow_{\epsilon_2}$ $\updownarrow_{\epsilon_d}$	$\theta_1=\pi/2$, $\phi_1=0$ $\theta_d=\phi_d=0$	175.259	50.666	28.90%	30.98%
IV	$\leftrightarrow_{\epsilon_1}$ $\updownarrow_{\epsilon_2}$ $\leftrightarrow_{\epsilon_d}$	$\theta_1=\theta_d=\pi/2$ $\phi_1=\phi_d=0$	190.815	−42.666	−22.36%	−22.65%
V	$\leftrightarrow_{\epsilon_1}$ $\updownarrow_{\epsilon_2}$ $\nearrow_{\epsilon_d}$	$\theta_1=\theta_d=\pi/2$ $\phi_1=0$, $\phi_d=\pi/2$	56.148	−8.00	−14.24%	−16.19%

ing a major part of the nonmodulated portion of the signal as well as experimental noise.

A second point demonstrated in Table I is that the quantum-beat modulation depth is very sensitive to the polarization configuration of the exciting pulses. The configuration with $\hat{\epsilon}_1$ perpendicular to $\hat{\epsilon}_2$ leads to greater beat contrast than with $\hat{\epsilon}_1$ parallel to $\hat{\epsilon}_2$. Given the complexity of this example, resulting in part from the large angular momenta involved, the physical interpretation of this result is not evident. One can, however, find a similar correlation between the polarizations of successive pulses by studying a much simpler system. In Fig. 4 are schematic diagrams for the sequential laser excitation of an atom from a $J=0$ ground state through a $J=1$ intermediate state to a $J=1$ final state. The application of a magnetic field would lift the degeneracy of the $J=1$ magnetic substates and lead to Zeeman quantum beats in the emission from the final state. For this system we consider the results of different laser polarization configurations.

We suppose initially that $\hat{\epsilon}_1$ and $\hat{\epsilon}_2$ are parallel. There are two possibilities of interest: $\hat{\epsilon}_1$ and $\hat{\epsilon}_2$ parallel to the axis of quantization specified by the magnetic field (π polarization) or $\hat{\epsilon}_1$ and $\hat{\epsilon}_2$ perpendicular to the quantization axis (σ polarization). As shown in Figs. 4(a) and 4(b) the selection rules $\Delta m=0$ for π polarization and $\Delta m=\pm1$ for σ polarization lead after two-laser excitations to population of a single final substate ($J=1$, $m=0$) and consequently to no quantum beats.

We next suppose that $\hat{\epsilon}_1$ and $\hat{\epsilon}_2$ are mutually orthogonal. There are again two cases of interest: $\hat{\epsilon}_1$ or $\hat{\epsilon}_2$ parallel to the quantization axis. As shown in Figs. 4(c) and (4d) the appropriate selection rules lead in both cases to a coherent population of two final substates ($J=1$, $m=\pm1$) and consequently to quantum beats. For this example the beats are in fact 100% modulated if one detects

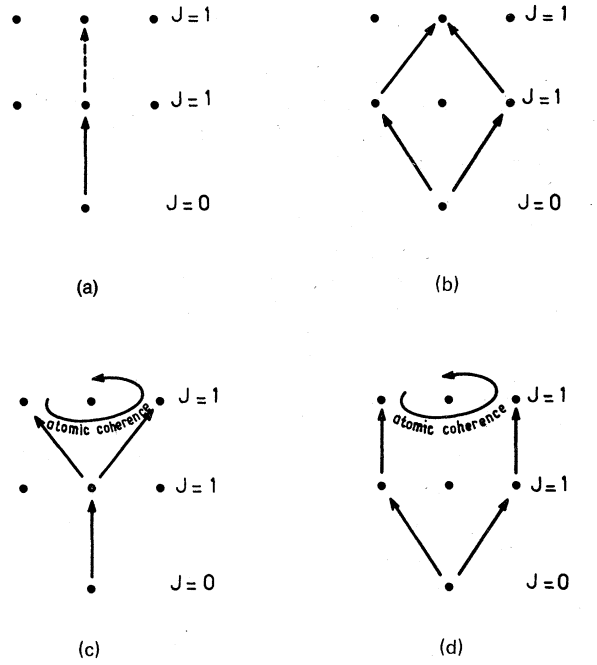

FIG. 4. Illustration of correlation between the generation of quantum beats and the polarization configuration of the exciting laser pulses for a simple atomic system. (a) $\hat{\epsilon}_1 \| \hat{\epsilon}_2 \| \hat{z}$, (b) $(\hat{\epsilon}_1 \| \hat{\epsilon}_2) \perp \hat{z}$, (c) $(\hat{\epsilon}_1 \perp \hat{\epsilon}_2)$; $\hat{\epsilon}_1 \| \hat{z}$, (d) $(\hat{\epsilon}_1 \perp \hat{\epsilon}_2)$; $\hat{\epsilon}_2 \| \hat{z}$, where $\hat{\epsilon}_1$ and $\hat{\epsilon}_2$ are the laser polarizations and $\hat{z}$ is the axis of quantization.

the signal with σ polarization [see Eq. (I13b)].

This simple example shows clearly that the relative orientation of the two excitation polarizations is very important and that greater beat contrast occurs for crossed polarizations. Although the experimental example of the sodium nD levels is more complex, this same conclusion remains qualitatively valid.

D. Effects of laser saturation in some simple cases

We now consider how laser saturation affects the results of Sec. IIC. To do this we will determine as an example the exact quantum-beat signal of the sodium nD levels for the polarization configuration III (see Table I). This configuration corresponds to the greatest modulation depth calculated within the framework of the weak pumping approximation.

In Fig. 5 is a diagram of all the levels involved in the excitation and decay processes with the corresponding transition matrix elements labeled. The polarization of the first laser pulse is perpendicular to the quantization axis $0Z$ (polarization σ); the selection rule $\Delta m_J = \pm 1$ is therefore applicable. From each sublevel of the $3S_{1/2}$ ground state there are two sublevels of the $3P_{3/2}$ intermediate-state excited:

$$3S_{1/2}(m_J = +\tfrac{1}{2}) \rightarrow 3P_{3/2}(m_J = -\tfrac{1}{2}, +\tfrac{3}{2}) ,$$

$$3S_{1/2}(m_J = -\tfrac{1}{2}) \rightarrow 3P_{3/2}(m_J = -\tfrac{3}{2}, +\tfrac{1}{2}) .$$

Each of these two pairs of $P_{3/2}$ sublevels is completely uncoupled from the other. The total system, at this point, can be regarded as a combination of two independent three-level systems such as treated in paper I, Sec. IIIA. As the sum of the transition probabilities $a_1^2 + b_1^2$ is the same for the two three-level systems, the density matrix of the system in the intermediate $3P_{3/3}$ state is independent of the saturation parameter of the first pulse [see Eq. I16) and the discussion following].

The second laser pulse is polarized parallel to the quantization axis (polarization π); therefore the selection rule $\Delta m_J = 0$ is applicable. From each sublevel of the $3P_{3/2}$ intermediate state one excites one sublevel (of the same m_J) in each of the two nD fine-structure components:

$$3P_{3/2}(m_J) \rightarrow nD_{3/2}(m_J), nD_{5/2}(m_J) .$$

For this excitation the resulting atomic system can be regarded as four independent three-level systems.[6] From symmetry considerations it is evident that the transition matrix elements are the same for excitation out of $3P_{3/2}(m_J = \pm\frac{3}{2};)$ likewise, for excitation out of $3P_{3/2}(m_J = \pm\frac{1}{2})$.

We have, therefore, only two distinct and independent three-level systems. The signal is obtained by doubling the contribution determined for these two systems. As shown in Fig. 5 the corresponding excitation matrix elements are a_2, b_2 for the first system and a_2', b_2' for the second.

To obtain the signal we must consider the transition matrix elements for spontaneous emission to the $3P$ levels. [See Figs. 5(b) and 5(c).] Transitions to the level $3P_{3/2}$ can originate from the $m_J = \pm\frac{3}{2}$ sublevels of $nD_{5/2}$ and $nD_{3/2}$ with respective amplitudes a_2 and b_2, or from the $m_J = \pm\frac{1}{2}$ sublevels of $nD_{5/2}$ and $nD_{3/2}$ with respective amplitudes a_2', b_2'. Transitions to the level $3P_{1/2}$ can originate only from the $m_J = \pm\frac{1}{2}$ sublevels of $nD_{3/2}$. This amplitude is designated c_2.

The exact quantum-beat signal follows from the analysis given in paper I, Sec. IIIA:

$$I = 2a_1^2 k_0^{(1)}(+\infty) k_0^{(2)}(+\infty)(a_2^4 + b_2^4 + 2a_2^2 b_2^2 \cos\omega_{FS} t) e^{-\Gamma t} + 2b_1^2 k_0^{(1)}(+\infty) k_0'^{(2)}(+\infty) \times (a_2'^4 + b_2'^4 + 2a_2'^2 b_2'^2 \cos\omega_{FS} t + a_2'^2 c_2^2) e^{-\Gamma t} , \quad (21a)$$

where

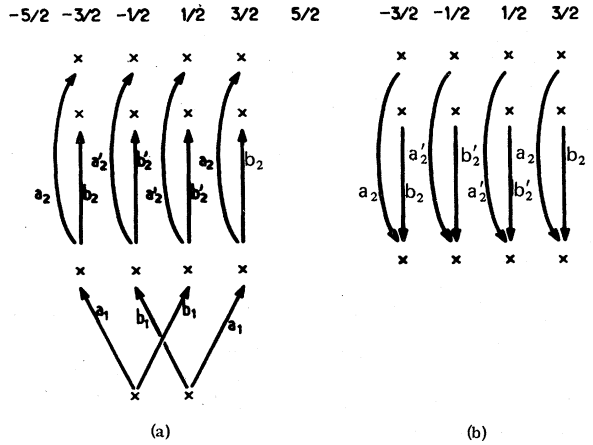

FIG. 5. Detailed level diagram, showing excitation and decay transition-matrix elements, for the two-laser echelon excitation of sodium nD Rdyberg states. (a) The first excitation leads to two uncoupled three-level systems. The second excitation leads to four uncoupled three-level systems. (b) Decay to the $3P_{3/2}$ level leads to four uncoupled three-level systems. (c) Decay to the $3P_{1/2}$ leads to two uncoupled two-level systems.

$$k_0^{(1)}(+\infty)=\frac{1}{2(a_1^2+b_1^2)}\times\left[1-\exp\left(-\int_{-\infty}^{+\infty}dt'\,\frac{2(a_1^2+b_1^2)}{T_p^{(1)}(t')}\right)\right],$$

$$k_0^{(2)}(+\infty)=\frac{1}{2(a_2^2+b_2^2)}\times\left[1-\exp\left(-\int_{-\infty}^{+\infty}dt'\,\frac{2(a_2^2+b_2^2)}{T_p^{(2)}(t')}\right)\right],$$

$$k_0'^{(2)}(+\infty)=\frac{1}{2(a_2'^2+b_2'^2)}\times\left[1-\exp\left(-\int_{-\infty}^{+\infty}dt'\,\frac{2(a_2'^2+b_2'^2)}{T_p^{(2)}(t')}\right)\right],\tag{21b}$$

with $a_1^2=3b_1^2=0.75$; $b_2^2=4a_2^2=8\times10^{-2}$; $c_2^2=50a_2'^2=11.11\times10^{-2}$; $b_2'^2=12\times10^{-2}$. The ratio $[k_0^{(2)}(+\infty)]/[k_0'^{(2)}(+\infty)]$ depends on the saturation parameter. If $S\equiv T/T_p\ll1$, then

$$\frac{k_0^{(2)}(+\infty)}{k_0'^{(2)}(+\infty)}=1\,.$$

If $T/T_p\gg1$, then

$$\frac{k_0^{(2)}(+\infty)}{k_0'^{(2)}(+\infty)}=\frac{a_2'^2+b_2'^2}{a_2^2+b_2^2}\,.$$

We see in this case that the beat signal depends on the saturation parameter of the second laser excitation. The numerical evaluation of the signal in the limit of strong pumping, leads in this case to an amplitude modulation of 30.99%. This is to be compared with 28.90% predicted by the theory in the weak-pumping approximation. The effect of laser saturation in this case is seen to be practically negligible. The last column of Table I gives, for the five polarization configurations, the value η_s of the beat-modulation depth in the case of strong pumping. Comparison with the weak-pumping parameter η_0 tabulated in the adjacent column shows that in all cases the effects of saturation are either null or extremely small.

III. QUANTUM BEATS PRODUCED BY SEQUENTIAL LASER EXCITATION IN THE PRESENCE OF AN EXTERNAL FIELD

A. General expression for the beat signal

In the preceding sections only couplings internal to the atom (e.g., fine or hyperfine structure) were responsible for the time evolution of off-diagonal elements of the excited-state density matrix (i.e., the precession of the analogous classical electric dipole moment) leading to the appearance of quantum beats in the decay radiation. We now generalize our theory to include the interaction of the atom with an external static electric or magnetic field. The external field lifts the degeneracy of the different magnetic sublevels of a given fine-structure or hyperfine-structure component thereby giving rise to new beat frequencies. The beats observed under these conditions permit one to measure important atomic parameters such as Landé g factors of polarizabilities.

To determine the time evolution of the atomic system we add to the field-free Hamiltonian $\mathcal{H}_0$, the Hamiltonian of the external interaction $\mathcal{H}_{ex}$ whose specific form differs according to whether an electric or magnetic field is involved. In the case of coupling to a magnetic field $\vec{B}_0$, $\mathcal{H}_{ex}$ in the absence of hyperfine structure can be written for a basis of states $|nLS\rangle$ as

$$\mathcal{H}_{ex}=-\frac{\mu_B\vec{B}_0}{\hbar}(\vec{L}+2\vec{S}),\tag{22}$$

where μ_B is the Bohr magneton. In the case of coupling to an electric field $\vec{E}$, $\mathcal{H}_{ex}$ can be written as an effective Stark Hamiltonian:

$$\mathcal{H}_{ex}=\sum_{n'L'J'm'}\frac{\vec{E}\cdot\vec{\mathfrak{D}}\,|n'L'J'm'\rangle\langle n'L'J'm'|\,\vec{E}\cdot\vec{\mathfrak{D}}}{E_{nLJ}-E_{n'L'J'}}\,.\tag{23}$$

To simplify the following analysis we let the direction of the external field and not the polarization ϵ_2 determine the quantization axis $0Z$. We assume that the external field is switched on adiabatically. The eigenstates of the Hamiltonian $\mathcal{H}_0+\mathcal{H}_{ex}$, designated $|Jm_j\rangle_{ex}$, evolve continuously from the eigenstates $|Jm_J\rangle$ of the field-free Hamiltonian. The time evolution of an atomic system can be determined once one knows the eigenvalues $E^{ex}_{Jm_J}$ of the Hamiltonian $\mathcal{H}_0+\mathcal{H}_{ex}$ and the projections $\langle Jm_J\,|J'm_{J'}\rangle_{ex}$ of the perturbed eigenvectors on the base of field-free eigenvectors. If, as is assumed here, the electric or magnetic interaction is invariant under rotation about $0Z$, the following relation is applicable:

$$\langle Jm_J\,|J'm_{J'}\rangle_{ex}=\delta_{m_Jm_J'}\langle Jm_J\,|J'm_J\rangle_{ex}\,.$$

We suppose that the diagonalization of $\mathcal{H}_0+\mathcal{H}_{ex}$ has already been effected by standard techniques, and now consider how one uses these results to generalize the quantum-beat signal, Eq. (18). We reconsider the analysis leading to the multipolar expansion of the signal and record below the step at which the hypothesis of no external fields was employed to obtain explicitly the beat frequencies

$$I = k_0^{(1)}(+\infty)k_0^{(2)}(+\infty)[(2J_0+1)(2J_f+1)]^{-1/2}e^{-\Gamma t}$$
$$\times {}^{J_f J_f}_{00}A^{J_2'' J_2''}_{k_2' q_2'}(\hat{\epsilon}_d^*)$$
$$\times \mathrm{Tr}\{{}^{J_2'' J_2'''}_{q_2' k_2'}T^{\dagger}\, e^{-\mathcal{H}_0 t/\hbar}\, {}^{J_2 J_2'}_{k_2 q_2}T\, e^{+i\mathcal{H}_0 t/\hbar}\}$$
$$\times {}^{J_2 J_2'}_{k_2 q_2}A^{J_1 J_1'}_{k_1 q_1}(\hat{\epsilon}_2)\,{}^{J_1 J_1'}_{k_1 q_1}A^{J_0 J_0}_{00}(\hat{\epsilon}_1). \qquad (24)$$

[Use of Eq. (3) for the time evolution of the irreducible tensor operators in the above equations leads immediately to Eq. (14).] To include the external field we now replace $\mathcal{H}_0$ by $\mathcal{H}_0+\mathcal{H}_{ex}$ in Eq. (24) and employ the definition of T_q^k to evaluate explicitly the trace Tr:

$$\mathrm{Tr} = \sum [(2k_2+1)(2k_2'+1)]^{1/2}(-1)^{J_2''-m+J_2-m'}\begin{pmatrix} J_2'' & k_2' & J_2''' \\ -m & q_2' & m-q_2' \end{pmatrix}\begin{pmatrix} J_2 & k_2 & J_2' \\ -m' & q_2 & m'-q_2 \end{pmatrix} \qquad (25)$$
$$\times \langle J_2'' m \mid e^{-(\mathcal{H}_0+\mathcal{H}_{ex})t/\hbar}\mid J_2 m'\rangle\langle J_2' m'-q_2 \mid e^{+i(\mathcal{H}_0+\mathcal{H}_{ex})t/\hbar}\mid J_2''' m-q_2'\rangle .$$

Since m_J remains a good quantum number, we have $m=m'$, and $q_2=q_2'$. By introducing the closure relations of the $|Jm_J\rangle_{ex}$ base and recognizing $|Jm_J\rangle_{ex}$ to be an eigenvector of $\mathcal{H}_0+\mathcal{H}_{ex}$ we obtain the following compact form for the quantum-beat signal:

$$I = k_0^{(1)}(+\infty)k_0^{(2)}(+\infty)[(2J_0+1)(2J_f+1)]^{-1/2}\exp[-i(\omega^{ex}_{Jm}-\omega^{ex}_{J'm-q_2})t]\exp(-\Gamma t)$$
$$\times {}^{J_f J_f}_{00}A^{J_2' J_2''}_{k_2' q_2}(\hat{\epsilon}_d^*)\,{}^{J_2'' J_2''}_{k_2' q_2}T^{J_2 J_2'}_{k_2 q_2}(J,J',m)\,{}^{J_2 J_2'}_{k_2 q_2}A^{J_1 J_1'}_{k_1 q_1}(\hat{\epsilon}_2)\,{}^{J_1 J_1'}_{k_1 q_1}A^{J_0 J_0}_{00}(\hat{\epsilon}_1), \qquad (26a)$$

where

$${}^{J_2'' J_2'''}_{k_2' q_2}T^{J_2 J_2'}_{k_2 q_2}(J,J',m)$$
$$= \sum [(2k_2+1)(2k_2'+1)]^{1/2}(-1)^{J_2''+J_2-2m}\begin{pmatrix} J_2'' & k_2' & J_2''' \\ -m & q_2 & m-q_2 \end{pmatrix}\begin{pmatrix} J_2 & k_2 & J_2' \\ -m & q_2 & m-q_2 \end{pmatrix}$$
$$\times \langle J_2'' m \mid Jm\rangle_{ex\,ex}\langle Jm \mid J_2 m\rangle\langle J_2' m-q_2 \mid J'm-q_2\rangle_{ex\,ex}\langle J'm-q_2 \mid J_2''' m-q_2\rangle . \qquad (26b)$$

There now appear in the signal terms modulated at frequencies corresponding to energy intervals between the different sublevels $|Jm_J\rangle_{ex}$.

The mathematical form of Eq. (26a) can be given a simple physical interpretation. The A coefficients describe from right to left the different excitation and detection processes. The T coefficients describe the processes of evolution within the excited state. These coefficients appear only between $A(\hat{\epsilon}_2)$ and $A(\hat{\epsilon}_d)$ because only state 2 has the time to evolve and it is this evolution that leads to the observed quantum beats. If the laser pulses do not follow each other in a time short compared with the time evolution of state 1 (as we have assumed throughout this analysis), the above formalism allows one to take this into account in a simple manner. One inserts between $A(\hat{\epsilon}_2)$ and $A(\hat{\epsilon}_1)$ coefficients of the form $Te^{i\omega\Delta t}$, where Δt represents the time interval between the two pulses.

B. Application to a particular case: Zeeman beats in the *nD* levels of sodium

We reconsider now the echelon excitation of sodium nD Rydberg states in order to examine the effect of a magnetic field on the quantum-beat signal. For the sodium atom, $S=\frac{1}{2}$; therefore $J=L\pm\frac{1}{2}=\frac{5}{2}$ or $\frac{3}{2}$ for the D states. The matrix effecting the transition from the field-free eigenstates $|Jm_J\rangle$ to the perturbed eigenstates $|Jm_J\rangle_{ex}$ decomposes into submatrices of order 1×1 or 2×2.

For $|m_J|=L+\frac{1}{2}$, $|Jm_J\rangle_{ex}$ is an eigenvector of $\mathcal{H}_0+\mathcal{H}_{ex}$ and one has without any further calculation

$$|L+\tfrac{1}{2}, L+\tfrac{1}{2}\rangle_{ex} = |L+\tfrac{1}{2}, L+\tfrac{1}{2}\rangle$$
$$= |L, S, m_L=L, m_s=\tfrac{1}{2}\rangle$$
$$|L+\tfrac{1}{2}, -L-\tfrac{1}{2}\rangle_{ex} = |L+\tfrac{1}{2}, -L-\tfrac{1}{2}\rangle$$
$$= |L, S, m_L=-L, m_S=-\tfrac{1}{2}\rangle . \qquad (27)$$

The eigenvalues follow immediately from the expression for $\mathcal{H}_{ex}$, Eq. (22) and from Eq. (27)

$$\omega^{ex}_{L+\frac{1}{2},\pm(L+\frac{1}{2})} = \tfrac{1}{2}AL \pm \omega_0(L+1) , \qquad (28a)$$

with

$$\omega_0 = -\mu_B B_0/\hbar . \qquad (28b)$$

For $|m_J| \leq L-\frac{1}{2}$ one must diagonalize a 2×2 matrix for each value of m_J. Introducing the angles $\theta_m(\omega_0)$ defined by

$$\tan\theta_m(\omega_0) = \frac{|A|[L(L+1)-(m+\frac{1}{2})(m-\frac{1}{2})]^{1/2}}{\omega_0+Am} , \qquad (29)$$

with

$$0 \leq \theta_m(\omega_0) < \pi$$

we can express $|J m_J\rangle_{ex}$ in the base $|LS m_L m_S\rangle$ by means of a simple rotation:

$$|L+\tfrac{1}{2}, m\rangle_{ex} = \cos[\tfrac{1}{2}\theta_m(\omega_0)]\,|m-\tfrac{1}{2}, \tfrac{1}{2}\rangle + \sin[\tfrac{1}{2}\theta_m(\omega_0)]\,|m+\tfrac{1}{2}, -\tfrac{1}{2}\rangle \quad (30a)$$

$$|L-\tfrac{1}{2}, m\rangle_{ex} = -\sin[\tfrac{1}{2}\theta_m(\omega_0)]\,|m-\tfrac{1}{2}, \tfrac{1}{2}\rangle + \cos[\tfrac{1}{2}\theta_m(\omega_0)]\,|m+\tfrac{1}{2}, -\tfrac{1}{2}\rangle\ . \quad (30b)$$

In the above equation it is understood that $L=2$, $S=\frac{1}{2}$, and only m_L, m_S are therefore explicitly shown in each vector $|LS m_L m_S\rangle$.

Since $|J m_J\rangle$ is obtained in the same manner for $\omega_0 = 0$, we have immediately

$$|L+\tfrac{1}{2}, m\rangle_{ex} = \cos\tfrac{1}{2}[\theta_m(\omega_0) - \theta_m(0)]\,|L+\tfrac{1}{2}, m\rangle + \sin\tfrac{1}{2}[\theta_m(\omega_0) - \theta_m(0)]\,|L-\tfrac{1}{2}, m\rangle\ , \quad (31a)$$

$$|L-\tfrac{1}{2}, m\rangle_{ex} = -\sin\tfrac{1}{2}[\theta_m(\omega_0) - \theta_m(0)]\,|L+\tfrac{1}{2}, m\rangle + \cos\tfrac{1}{2}[\theta_m(\omega_0) - \theta_m(0)]\,|L-\tfrac{1}{2}, m\rangle\ , \quad (31b)$$

with

$$L-\tfrac{1}{2} \leq m \leq L+\tfrac{1}{2}\ .$$

The eigenvalues corresponding to the basis vectors $|J m_J\rangle_{ex}$ are easily shown to be

$$\omega^{ex}_{L\pm 1/2, m} = -\tfrac{1}{4}A + \omega_0 m \pm \tfrac{1}{2}[(Am+\omega_0)^2 + A^2(L(L+1) - (m+\tfrac{1}{2})(m-\tfrac{1}{2}))]^{1/2}\ . \quad (32)$$

Figure 6 shows the variation of the energy levels as a function of the applied magnetic field B_0.

Since the perturbed eigenvectors and eigenvalues are now known, the quantum beat signal, Eq. (26), can be completely determined. We performed this calculation numerically for the different Bohr precession frequencies of the system; the results are summarized graphically in Figures 7–9 for the respective experimental conditions of zero field, weak field ($\omega_0 \ll A$), and strong field ($\omega_0 \gg A$). The polarization configuration is one for which ϵ_1, ϵ_2, and ϵ_d are parallel to each other and perpendicular to B_0.

For the case of zero field (Fig. 7), one obtains a beat frequency corresponding to the fine-structure level separation $\omega_{FS} = \frac{5}{2}A$ with a very weak modulation depth as expected. (See Table I, case I.)

In the case of a weak magnetic field (Fig. 8), the fluorescence is modulated primarily at the frequency $2.4\ \mu_B B_0$ which corresponds to twice the Larmor frequency of the $D_{5/2}$ level. (The Landé factor is $g_J = 1.2$.) The calculation shows that in this case the signal is particularly sensitive to the $\Delta m_J = 2$ coherence in the $D_{5/2}$ level. [See arrows in the low-field region of Fig. 6.] The contributions of other coherence terms (either within the $D_{3/2}$ level or between the $D_{3/2}$ and $D_{5/2}$ levels) evolving at different frequencies are very weak.

The measurement of Zeeman beats in a weak magnetic field therefore provides directly the Landé g factor of the $D_{5/2}$ level. In the case of a strong magnetic field (Fig. 9), the analytic form of the signal is

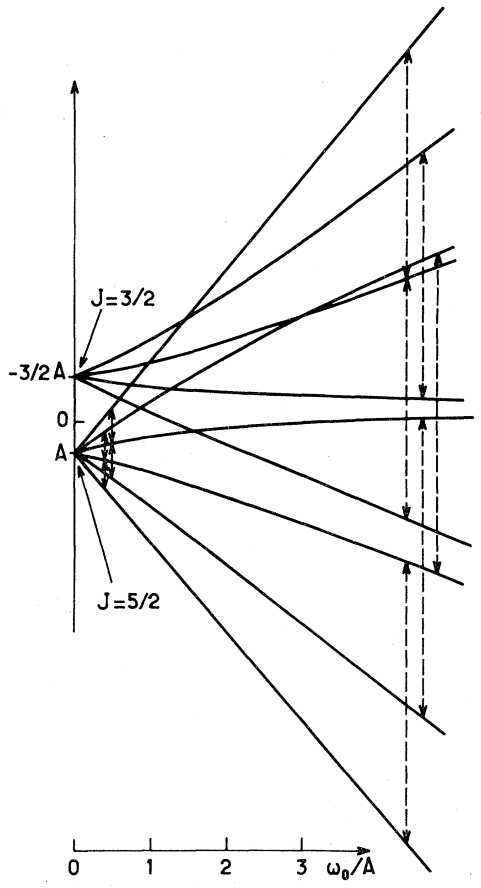

FIG. 6. Energy variation of the nD sublevels as a function of the external magnetic field. Arrows indicate the expected quantum-beat frequencies in the regions of low field and high field.

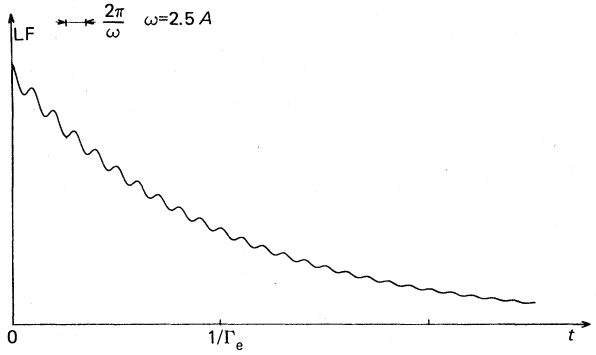

FIG. 7. Theoretical zero-field quantum-beat signal.

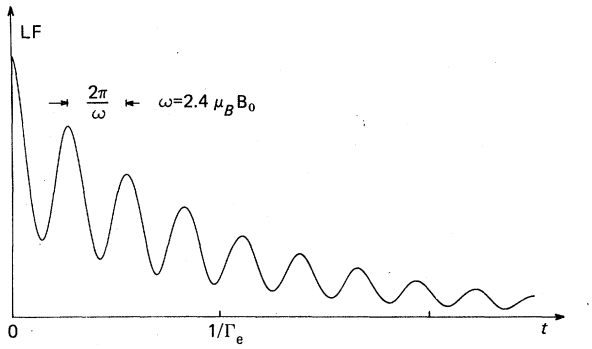

FIG. 8. Theoretical weak-field ($\omega_0 \ll A$) quantum-beat signal.

$$I = 198.15 + 105.55\cos(At)\cos(2\omega_0 t)\,. \qquad (33)$$

The signal therefore consists of a carrier wave at the frequency $2\omega_0 = 2\mu_B B_0/\hbar$ modulated at the frequency A corresponding to the fine-structure interaction parameter. The two frequencies appearing in the signal are indicated by arrows on the high-field region of Fig. 6. A simple interpretation can be given to this result in terms of the classical vector model. For a high magnetic field the angular momenta $\vec{L}$ and $\vec{S}$ are decoupled and one observes essentially the free precession of the orbital angular momentum about the magnetic field. This explains the appearance of the Larmor frequency $2\mu_B B_0/\hbar$ in place of $2.4\mu_B B_0/\hbar$. One must also take into account, however, the contribution of the diagonal part $Am_L m_S$ of the fine-structure Hamiltonian $A\vec{L}\cdot\vec{S}$. This acts as a perturbation adding to the applied field the small internal field $B' = Am_S/\mu_B$, which may be positive or negative according to the sign of m_S. There are therefore two Larmor frequencies $2\mu_B B_0/\hbar = (2\mu_B/\hbar)[B_0 \pm (A/2\mu_B)]$. The sum of two cosinusoidal terms at these frequencies gives the frequency dependence of Eq. (33):

$$\cos[(2\mu_B/\hbar)(B_0 + A/2\mu_B)t] + \cos[(2\mu_B/\hbar)(B_0 - A/2\mu_B)t] = 2\cos(At)\cos(2\mu_B/\hbar)B_0 t)\,.$$

The above quantum-beat experiment suggests a new way to measure the fine-structure interaction constant. Instead of measuring the beats in zero field, one applies a strong field to decouple $\vec{L}$ and $\vec{S}$ and measures the frequency of the envelope of the Zeeman beats (Fig. 9). As seen from the particular case treated here, there is a marked enhancement in the signal-to-noise ratio.

IV. CONCLUSION

The theory of laser-induced quantum beats introduced in paper I has been further developed to include the effects of echelon excitation by several lasers for field-free atomic systems as well as for atoms subjected to external static fields. A detailed study was made of the dependence of the

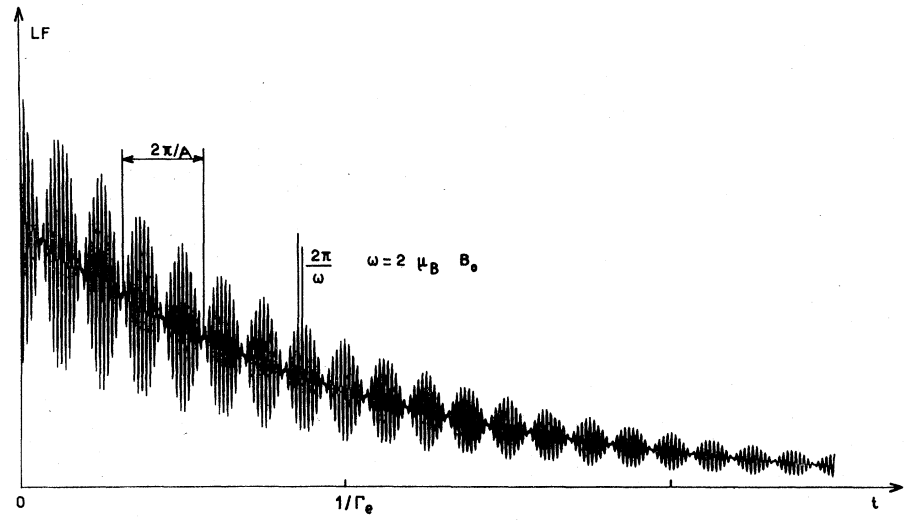

FIG. 9. Theoretical strong-field ($\omega_0 \gg A$) quantum-beat signal.

quantum-beat signal on the polarization configuration of the exciting light and the detected fluorescence. The use of spherical tensor operators permitted one to show the explicit angular dependences of different multipolar contributions to the signal. When evaluated within the framework of the linear or weak-pumping approximation, the signal was expressible in a mathematical form easily interpreted in terms of the different excitation and detection processes involved and easily generalized to include any number of laser excitations. Application of the theory to systems of experimental interest showed in the case of two-laser excitation that greatest amplitude modulation of the fluorescence occurred for orthogonal laser polarizations. A reexamination using the rigorous results of the general theory showed that laser saturation effects modified the weak pumping calculation to a very small extent. The analysis of Zeeman beats produced by echelon excitation of sodium nD Rydberg states in the presence of a magnetic field led to a new experimental idea: the measurement in high magnetic field of the frequency of the envelope of the quantum-beat signal as a means of determining the fine-structure interaction parameter.

---

[1]M. P. Silverman, S. Haroche, and M. Gross, Phys. Rev. A 18, 1507 (1978), preceding paper.

[2]S. Haroche, M.Gross, and M. Silverman, Phys. Rev. Lett. 33, 1063 (1974); C. Fabre, M. Gross, and S. Haroche, Opt. Commun. 13, 393 (1975).

[3]Equations referred to in paper I will be prefixed by I.

[4]A. Messiah, *Mécanique Quantique, Tome II*, (Dunod, Paris, 1964). For application of irreducible tensors to optical pumping problems, see, for example, A. Omont, J. Phys. (Paris) 26, 26, 576 (1965); or W. Happer, Rev. Mod. Phys. 44, 169 (1972).

[5]M. Gross, Thèse de 3 ème cycle (Paris, 1975) (unpublished).

[6]Actually, there exist in the $P_{3/2}$ level off-diagonal density-matrix elements between the $m_J=\frac{3}{2}$ and $m_J=-\frac{1}{2}$ substates and between the $m_J=-\frac{3}{2}$ and $m_J=\frac{1}{2}$ substates. We neglect this throughout the analysis. This is justified because the second laser excitation of π polarization couples these density-matrix elements to $\Delta m_J=2$ density-matrix elements of the nD manifold. These coherence terms will not be detected, however, since the detected fluorescence is also π polarized and therefore sensitive only to $\Delta m_J=0$ coherence terms of the excited states.